

Optimal Control for Geometric Motion Planning of a Robot Diver

Roberto Shu¹, Avinash Siravuru², Akshara Rai¹, Tony Dear¹, Koushil Sreenath², and Howie Choset¹

Abstract—Inertial reorientation of airborne articulated bodies has been an active area of research in the robotics community, as this behavior can help guide dynamic robots to a safe landing with minimal damage. The main objective of this work is emulating the aggressive and large angle correction maneuvers, like somersaults, that are performed by human divers. To this end, a planar three link robot, called DiverBot, is proposed. By considering a gravity-free scenario, a *local connection* is obtained between joint angles and the body orientation, resulting in a reduction in the system dynamics. An optimal control policy applied on this reduced configuration space yielded diving maneuvers that are dynamically feasible. Numerical results show that the DiverBot can execute one somersault without drift and multiple somersaults with minimal drift.

I. INTRODUCTION

Mid-air reorientation is an exciting domain of research for roboticists, who are currently trying to achieve this behavior in robots of various morphologies [1]–[5]. Animals use this ability to self-right their orientations during free-falls to protect themselves from severe, and sometimes fatal, injuries. Once robots leave the protective and controlled research lab environments and go outdoors, it would be imperative for them to know how to fall in ways that cause minimal damage.

The main aim of this work is to achieve large mid-air reorientation maneuvers using a planar three-linked robot, called DiverBot, which is modeled after a human diver. Though diving is not necessarily a damage control action, the maneuver serves as an ideal benchmark to characterize the quick reorienting power of any control law developed for a human-like robot. While humans have a remarkable ability to naturally perform multiple flips during the diving manoeuvre, the underlying biological control is not fully understood, and therefore hard to emulate in robots.

The falling cat problem is probably the most popular and well-studied instance of mid-air reorientation from the animal kingdom, specifically of releasing with zero angular momentum (also called *drift-less*) and allowing the use of only internal body shape changes. Kane and Scher [6] proposed the first dynamical solution to this problem, while Montgomery [7] explained this manoeuvre in further detail using the concept of a *local connection*. This local connection relates the shape changes of cat’s limbs to the net rotation of its body, as a consequence of the conservation of

net angular momentum [8], [9]. When seen from this standpoint, such systems are classical examples of non-holonomic systems, whose motion planning has been explored in the controls community in the past [10]–[12].

Similarly, human diving action could also be explained by invoking the conservation of angular momentum [13]. Modeling and control of human diving were also studied within the robotics and control community. In [14], the diving is divided into phases and appropriate control laws are used in each phase. On the contrary, in both [15] and [16], the non-holonomic nature of the system is exploited to propose simple learning-based and bang-bang control laws, respectively. Finally, a successful implementation of a somersault, using a 3D biped was demonstrated in [17], using a phased controller and launching from the ground with non-zero momentum. While all these controllers provide valid solutions, they do not comment on the optimality of the maneuver. More recently however, sensorimotor control theories have emerged which conclude that our movement coordination does indeed seek to achieve an *optimal performance* [18], [19]. Some optimal control formulations have been proposed for diving in the past [20]–[22], albeit without explicitly exploiting the local connection.

The key contribution for this work is a systematic approach to synthesize the more analytical tools from develop geometric mechanics with optimal control in order to generate human-like diving as a single end-to-end motion. This allows us to posit that the naturally occurring human diving maneuver is an optimal response to the rapid mid-air reorientation problem. Moreover, we leverage the reduced form of the system dynamics to generate a smaller optimization problem and thus improve speed of convergence to a feasible solution. A systematic method to derive the reduced dynamics and pose an optimal control problem is provided.

The rest of the paper is organized as follows. Section II introduces the robot model and the corresponding local connection is derived. In Section III, the optimal control problem is formulated for the diving motion. Section IV summarizes key numerical simulation results. Finally, Section V provides conclusions and directions for future work.

II. MODEL DESCRIPTION

For this study, we limit our exploration of diving to the planar case, to first characterize the dominant behavior along the sagittal plane. Moreover, the hand and leg are modeled as single links without the elbow and knee joints, respectively. Note that, reorientations are harder (more expensive) with this configuration as greater torque needs to be applied at the hip and shoulder joints for reducing inertia, during the

¹Authors are with the Robotics Institute, Carnegie Mellon University, Pittsburgh, PA 15231, USA {rshum, arai, tonydear, choset}@cmu.edu

²Authors are with the Department of Mechanical Engineering, Carnegie Mellon University, Pittsburgh, PA 15231, USA {avinashs, koushils}@cmu.edu

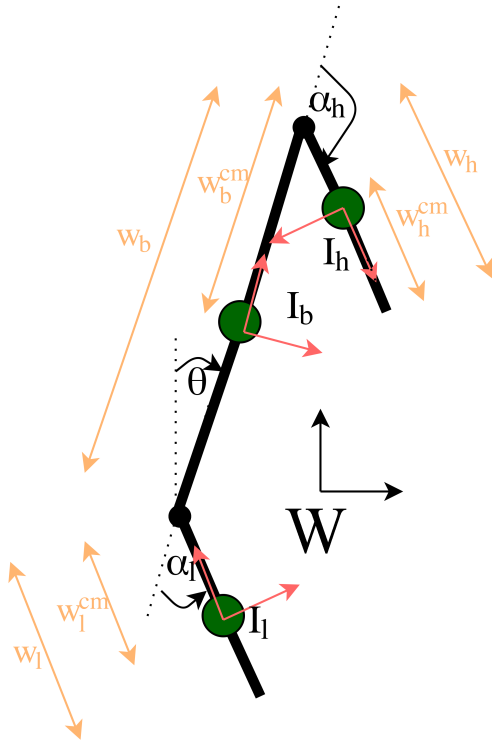


Fig. 1: A planar three link diver model

maneuver. In this case, there is also a possibility for the system center of mass (CoM) to drift further away from the body link CoM. However, an optimal solution to the three-link model guarantees the existence of a feasible solution to its five link counterpart, and it also serves as an ideal initial seed to search for an optimal policy in that high dimensional space.

The robot model, as shown in Fig. 1, has a configuration manifold which is $Q \in \text{SO}(2) \times (\mathbb{S}^1)^2 \times \mathbb{R}^2$. Fixing the body-fixed frame on $link_b$ (body link), its orientation and positions along x - and y -axes are defined w.r.t the ground inertial frame W as θ , x , y , respectively. The relative orientations

Notation	Definition
W	Inertial fixed frame
L_h	Body frame fixed at the CoM of $link_h$
L_l	Body frame fixed at the CoM of $link_l$
B	Body frame fixed at the CoM of $link_b$
$\theta \in \text{SO}(2)$	Orientation from W to B
$\alpha_h \in \mathbb{S}^1$	Orientation from B to L_h
$\alpha_l \in \mathbb{S}^1$	Orientation from B to L_l
$u_i \in \mathbb{R}$	Torque applied at $link_i$
i	Index to denote hand (h), body (b) and leg (l) links
$m_i \in \mathbb{R}$	Mass of $link_i$
$I_i \in \mathbb{R}^{3 \times 3}$	Inertia Matrix of $link_i$ in body frame
$w_i \in \mathbb{R}$	Length of $link_i$
$w_i^{com} \in \mathbb{R}$	Distance to the CoM of $link_i$ from its top end.

TABLE I: Notations used in this section and their definitions

of $link_h$ (hand) and $link_l$ (leg) are given by α_h and α_l , respectively. Only the relative joints α_1 and α_3 can be controlled, making the system an under-actuated one. All system parameter definitions and notations are summarized in Table I.

Using the generalized coordinates, $\mathbf{q} = [x \ y \ \alpha_h \ \theta \ \alpha_l]^T$, we define the Lagrangian, $L(\mathbf{q}, \dot{\mathbf{q}}) = T - V$, where T and V are the kinetic and potential energies of the system respectively.

$$T = \sum_i^{h,b,l} \frac{1}{2} m_i \dot{\mathbf{x}}_i^2 + \frac{1}{2} I_h \dot{\alpha}_h^2 + \frac{1}{2} I_b \dot{\theta}^2 + \frac{1}{2} I_l \dot{\alpha}_l^2 \quad (1)$$

$$V = \sum_i^{h,b,l} m_i g y_i \quad (2)$$

Here, g denotes acceleration due to gravity, and $\mathbf{x}_i = [x_i \ y_i]^T$, where x_i and y_i denote the CoM position of $link_i$. Hereafter, we neglect the translational dynamics of the body CoM, i.e. $\dot{\mathbf{x}}_b = [\dot{x} \ \dot{y}]^T = 0$, to focus only on the dynamics of reorientation. This reduces the configuration space to $Q_r \in \text{SO}(2) \times (\mathbb{S}^1)^2$. Using the principle of least action, the dynamics of the system are derived and represented in the compact form below:

$$\mathbf{D}(\mathbf{q}_r) \ddot{\mathbf{q}}_r + \mathbf{C}(\mathbf{q}_r, \dot{\mathbf{q}}_r) + \mathbf{G}(\mathbf{q}_r) = \mathbf{B} \mathbf{u} \quad (3)$$

where, $\mathbf{B} = \begin{bmatrix} 1 & 0 \\ 0 & 0 \\ 0 & 1 \end{bmatrix}$, $\mathbf{q}_r = [\alpha_h \ \theta \ \alpha_l]^T$ and $\mathbf{u} = [u_h \ u_l]^T$.

We can see that, if $\mathbf{G}(\mathbf{q}_r) = 0$, i.e. if the potential energy is neglected, then it can be easily seen that the Lagrangian is independent of θ . In other words, the Lagrangian has a symmetry group \mathbb{S}^1 , implying an invariance to changes in θ . Similar to [15], for the rest of this study, we assume that the effects of gravity on θ are minimal and thus neglect potential energy. However, for a given drop height, the resulting time of flight can be used to determine the desired average body velocity, θ_{avg}^d . This can be strictly enforced in the optimal control problem.

As a result of the invariance, Noether's theorem predicts the conservation of a quantity, which is the diver's angular momentum in this case.

$$\frac{\partial L}{\partial \theta} = 0 \quad \text{and} \quad \frac{d}{dt} \frac{\partial L}{\partial \dot{\theta}} = 0 \quad (4)$$

Therefore, $\frac{\partial L}{\partial \dot{\theta}} = p$. Substituting p in (3) followed by some computations gives,

$$p = \mathbb{I}_\theta(\alpha) \dot{\theta} + \mathbb{I}_\alpha(\alpha) \dot{\alpha} \quad (5)$$

$$\dot{\theta} = -\mathbb{I}_\theta(\alpha)^{-1} \mathbb{I}_\alpha(\alpha) \dot{\alpha} + \mathbb{I}_\theta(\alpha)^{-1} p \quad (6)$$

where $\alpha = [\alpha_h \ \alpha_l]$. Equation (6) is called the *reconstruction equation* in the geometric mechanics community [8]. Additionally, $-\mathbb{I}_\theta(\alpha)^{-1} \mathbb{I}_\alpha(\alpha)$ and $\mathbb{I}_\theta(\alpha)$ are the local forms of the *mechanical connection*, compactly denoted as $\mathbf{A}_\theta(\alpha)$, and *locked inertia tensor*, respectively. It can easily be verified that both the local connection and the locked inertia tensor only depend on the shape variables, $(\alpha, \dot{\alpha})$.

Substituting Eqn. (6) in (3) gives the reduced set of equations of motion, as shown below.

$$\begin{aligned} \dot{\theta} &= \mathbf{A}_\theta(\boldsymbol{\alpha})\dot{\boldsymbol{\alpha}} + \mathbb{I}_\theta(\boldsymbol{\alpha})^{-1}p \\ \mathbf{D}_\alpha\ddot{\boldsymbol{\alpha}} &= -\mathbf{C}_\alpha(\boldsymbol{\alpha}, \dot{\boldsymbol{\alpha}}) + \mathbf{B}_\alpha\mathbf{u} \end{aligned} \quad (7)$$

Here, $\mathbf{D}_\alpha, \mathbf{C}_\alpha$ are the Inertia and Coriolis matrices corresponding only to the dynamics of the relative shape changes. Correspondingly, the reduced input matrix is $\mathbf{B}_\alpha = \begin{bmatrix} 1 & 0 \\ 0 & 1 \end{bmatrix}$. The components of $\mathbb{I}_\theta(\boldsymbol{\alpha}), \mathbb{I}_\alpha(\boldsymbol{\alpha}), \mathbf{D}_\alpha, \mathbf{C}_\alpha$, can be found in the Appendix. In the next section, we formulate an optimal control problem on these reduced dynamics with an objective to achieve flips with least control effort.

III. OPTIMAL CONTROL FORMULATION

A. Optimization Problem Formulation

Without loss of generality, we can rewrite (7) as a set of first-order equations:

$$\dot{\theta} = \mathbf{A}_\theta(\boldsymbol{\alpha})\dot{\boldsymbol{\alpha}} + \mathbb{I}_\theta(\boldsymbol{\alpha})^{-1}p \quad (8)$$

$$\dot{\alpha}_h = u_h \quad (9)$$

$$\dot{\alpha}_l = u_l \quad (10)$$

Note that, in Equations (7) there are three states (two of them are independent) and two control inputs in the dynamics of the DiverBot. The objective of performing flips can be articulated in the optimal control language as finding the control inputs $\mathbf{u}(t) = [u_h(t), u_l(t)]$, in the timespan $t \in [t_I, t_F]$, that will drive the system from an initial configuration $\mathbf{y}_I = \mathbf{y}(t_I) = [\theta_I, \alpha_{h,I}, \alpha_{l,I}, \dot{\alpha}_{h,I}, \dot{\alpha}_{l,I}]^T$ to a desired final configuration $\mathbf{y}_F = \mathbf{y}(t_F) = [\theta_d, \alpha_{h,d}, \alpha_{l,d}, \dot{\alpha}_{h,I}, \dot{\alpha}_{l,I}]^T$. Accordingly, we pose the optimal control problem to find an admissible time history of the control input $\mathbf{u}(t), t \in [t_I, t_F]$ as:

$$\min_{\mathbf{y}, \mathbf{u}} \mathbf{J}(\cdot) = \Phi(\mathbf{y}_F) + \int_{t_0}^{t_F} \mathcal{L}(\mathbf{y}(t)) dt \quad (11)$$

subject to:

$$\mathbf{H}(\mathbf{y}(t_I), \mathbf{y}(t_F)) = 0 \quad (12)$$

$$\mathbf{G}(\mathbf{y}(t), \mathbf{u}(t)) \leq 0 \quad (13)$$

where $\Phi(\cdot)$ is the terminal cost, $\mathcal{L}(\cdot)$ is the running cost. $\mathbf{H}(\cdot)$ are equality constraints that enforce system dynamics and boundary conditions. $\mathbf{G}(\cdot)$ are nonlinear inequality constraints that define joint angle and torque limits. For the problem to be solvable we assume that $\mathbf{J}(\cdot), \mathbf{H}(\cdot), \mathbf{G}(\cdot)$ are all smooth functions.

B. Discretization

The optimal control problem can be seen as a Nonlinear Programming (NLP) problem with an infinite number of variables [23]. To be numerically tractable, discretize the problem to obtain a finite-dimensional approximation, using N collocation points such that,

$$t_I = t_0 < t_1 < \dots < t_{N-1} = t_F. \quad (14)$$

For ease of notation we represent the value of state variables at each time step as $\mathbf{y}^k \equiv \mathbf{y}(t_k)$ for $k = 0, 1, \dots, N-1$, and similarly for the others. We chose a trapezoidal integration scheme with time-steps of length h to transcribe the dynamics from Equation (8) to (10) to obtain the following equality constraints:

$$(\theta^{k+1} - \theta^k) - \frac{h}{2} (\dot{\theta}^{k+1} + \dot{\theta}^k) = 0 \quad (15)$$

$$\dot{\theta}^{k+1} - (A(\boldsymbol{\alpha}^{k+1})\dot{\boldsymbol{\alpha}}^{k+1} + I^{-1}(\boldsymbol{\alpha}^{k+1})p) = 0, \quad (16)$$

$$(\boldsymbol{\alpha}^{k+1} - \boldsymbol{\alpha}^k) - \frac{h}{2} (\mathbf{u}^{k+1} + \mathbf{u}^k) = 0. \quad (17)$$

Additionally, the corresponding inequality constraints that represent joint and input limits are defined as:

$$\alpha_i^{min} \leq \alpha_i^k \leq \alpha_i^{max}, \quad (18)$$

$$\dot{\alpha}_i^{min} \leq \dot{\alpha}_i^k \leq \dot{\alpha}_i^{max}, \quad (19)$$

$$u_i^{min} \leq u_i^k \leq u_i^{max}. \quad (20)$$

where $k \in \{0, \dots, N-1\}$ and $i \in \{h, l\}$.

C. Implementation

We leveraged the *interior-point* algorithm from MATLAB's Optimization Toolbox [24], to solve the proposed optimal control problem on the discretized and reduced dynamics. We run two passes of our optimization with increasing grid size, $N_{\text{grid}} \in \{15, 50\}$ and limit to a maximum of 3000 iterations per pass. Like any non-linear constrained optimization problem, the minimum obtained is only locally optimal. More interestingly, this optimizer doesn't necessarily require the initial seed to be dynamically feasible. The algorithm covers fairly quickly even with a random guess. In the next section, the various numerical experiments conducted and their results are summarized.

IV. RESULTS AND DISCUSSION

A. Experiment setup

We strictly constrain the final time t_F to be equal to the time of flight t_{fall} for any given initial height h_0 as shown in (21). Additionally, joint and actuator limits in summarized in Table II while the model parameters are provided in Table III. Note that, the model parameters are determined from the rigid-body model of a human diver, presented in [14], by lumping it into only three segments (hand, torso, leg).

$$t_F \leq t_{\text{fall}} \Rightarrow t_F \leq \sqrt{\frac{2h_0}{g}} \quad (21)$$

We consider the planar diver reorientation problem under two scenarios. One is where the system starts at rest with no

TABLE II: State and Input Limits

	α_1	α_2	u_1, u_2
min	0	0	-1500
max	π	$\frac{2}{3}\pi$	1500

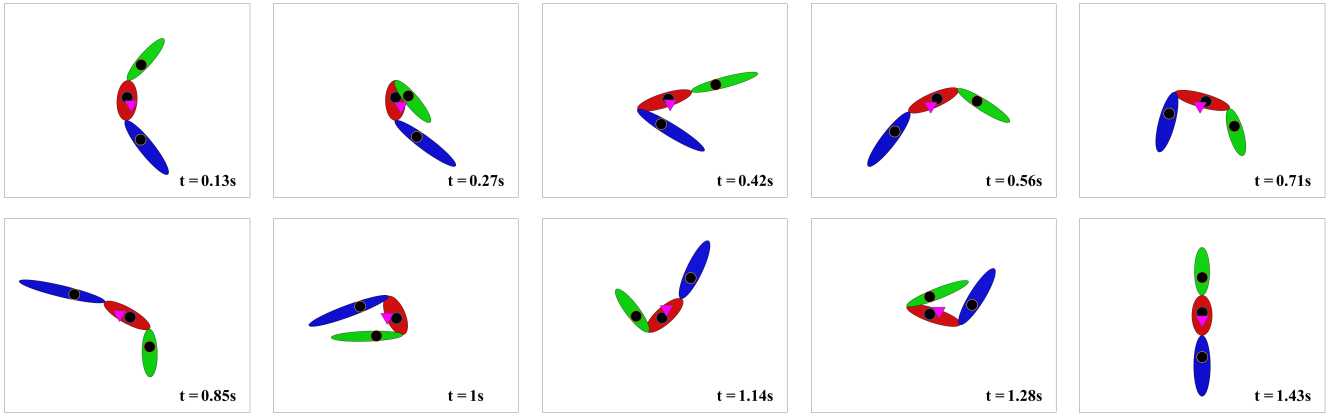


Fig. 2: Snapshots of DiverBot reorienting to perform a somersault simulation when dropped from a height of 10m without drift .

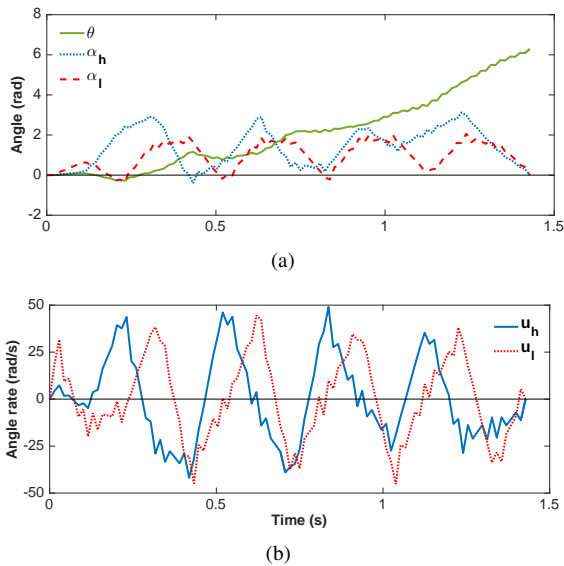


Fig. 3: Plots of the optimal (a) body orientation and shape change trajectories, (b) control input profiles for the drift-free case

angular velocity (i.e. drift-free). In this case the system is said to be a *purely mechanical system* [8]. In the second case, we consider a system with some initial angular velocity $\dot{\theta}_0$ (i.e. with drift). As a final test, we apply the optimal joint angle velocities obtained through a feed-forward control input to a system with gravity that more accurately models a human diver.

B. Drift-free Somersault

To perform a single somersault, we desire the robot to start from $y_I = [0 \ 0 \ 0 \ 0 \ 0]$ and get to $y_F = [2\pi \ 0 \ 0 \ 0 \ 0]$. Assuming the robot is dropped from height of 10m, the robot has only ≈ 1.4 s to achieve the reorientation before hitting the ground. In this case the robot starts with zero angular momentum. The optimal flip maneuver is shown in Fig. 2, and the corresponding joint input and displacement profiles

TABLE III: Physical Properties of the DiverBot

Property	Value (units)
m_b	45.88 kg
m_l	13.85 kg
m_h	4.45 kg
I_b	1.9155 kg-m ²
I_l	0.9753 kg-m ²
I_h	0.1579 kg-m ²
w_b	0.553 m
w_l	0.837 m
w_h	0.66 m
w_b^{com}	0.2369 m
w_l^{com}	0.2976 m
w_h^{com}	0.2441 m

are plotted in Fig. 3.

The hand and leg links oscillate out-of-phase to create a geometric phase, i.e., they cause a net rotation in θ . This behavior is very similar to the snake robot locomotion studied in [9], where the local connection is due to the no-drift frictional constraints as opposed to angular momentum conservation.

C. Two Somersaults with Initial Drift

In this case, the robot starts with some initial drift. We require the robot to go from $y_I = [0 \ 0 \ 0 \ 0 \ 0]$ and get to $y_F = [4\pi \ 0 \ 0 \ 0 \ 0]$, thus accomplishing two somersaults. There is a non-zero initial body velocity, $\dot{\theta}_0 \approx 4$ rad/s. Snapshots of the diving manoeuvre are shown in Fig. 4, while the joint and input profiles are shown in Fig. 5.

These motion profiles appear human-like. There is a compression phase that reduces the moment of inertia, then that shape is maintained for leveraging the higher rotation rate for the longest possible time, and finally they end with decompression phase to reduce the joint rates and re-orient to the desired final configuration.

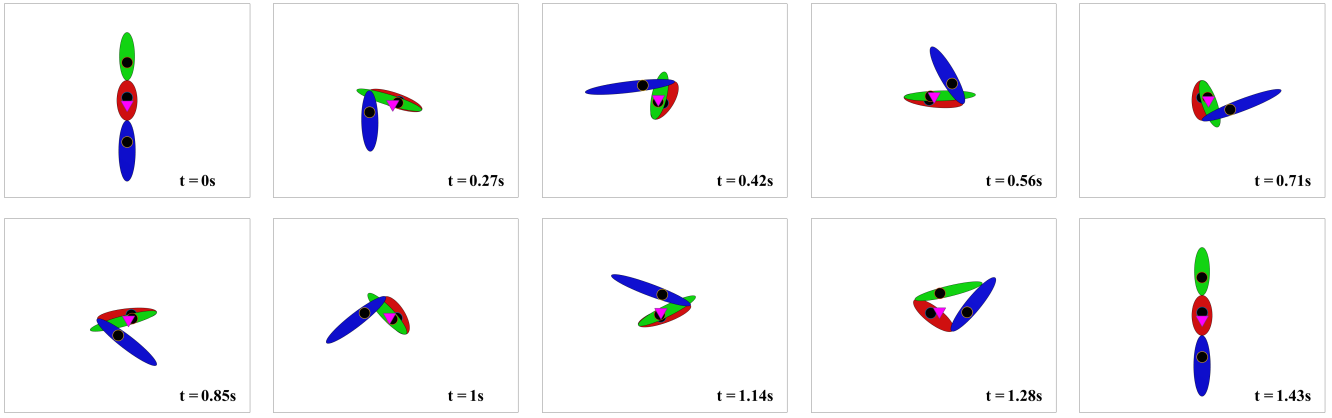


Fig. 4: Snapshots (with a time stamp) showing the DiverBot rapidly reorienting to perform two somersaults when launched with initial drift in the form of non-zero body angular velocity.

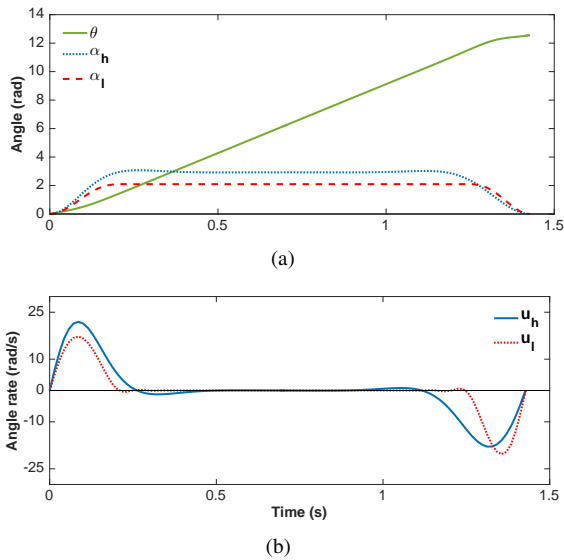


Fig. 5: Plots of the optimal (a) body orientation and shape change trajectories, (b) input profiles for the case with initial drift.

D. Discussion

All simulation results are generated on a 64-bit system using a Intel Core i7 2.66GHz machine with 8GB of RAM. Starting with a random initial seed for both cases, it still managed to find feasible and locally optimum solutions. In the case with drift the optimizer converged to a solution in less than a minute, while in the drift-free case convergence speed decreased and took approximately three minutes.

Overall, it can be seen that starting with a drift-free configuration requires much greater torques to perform a somersault. This is understandable as the hand and leg links, which have significantly smaller inertia than the body, have to expend enough to move the body link through a complete turn in a very short time. Moreover, the limited effectiveness of the inputs can be seen in the local connection (8). On the other hand, starting with some initial drift helps the process,

and the leg and hand links move to only reduce the system's inertia rather than to generate the rotation. Decreasing the system inertia will consequently increase $\dot{\theta}$ appropriately and achieve the desired reorientation within the desired time limit.

In Figs. 2 and 4, the CoM positions of the links are depicted with black circular markers, and the CoM of the DiverBot is also shown with pink triangular marker. It can be seen that during both the reorientation maneuvers, DiverBot's CoM does not go very far off the body link. The lesser its excursion, the more valid our assumption becomes of explicitly decoupling the translational and rotational dynamics of the DiverBot.

V. CONCLUSIONS AND FUTURE WORK

In this paper, we demonstrate rapid mid-air reorientation maneuvers for the DiverBot, which is modeled after a human diver. A reduction in the dynamics was obtained from the conservation of angular momentum. Using the reduced dynamics an optimal control problem was formulated. For the DiverBot example multiple dynamically feasible joint angle input trajectories were found to perform somersaults both with and without drift. More importantly, optimal input trajectories were found in less than a minute starting from a suboptimal infeasible initial trajectory seed.

The biggest drawback for this work is performing somersaults in the absence of gravity. However, we are able to achieve the reorientations strictly within the time of flight, which atleast offers a feasible trajectory. At this point, we conjecture that any resulting variation in the presence of gravity would be minor and, if required, it could be corrected with a simple PD-based tracking controller. Therefore, immediate future work involves validating these ideas in the presence of gravity when $G(q) \neq 0$. Additionally, we intend to build a small prototype with similar mass distribution to test these optimal policies on a real robot.

APPENDIX

The components of the DiverBot dynamics, as described in 7, are provided below:

$$\begin{aligned}
\mathbb{I}_\theta(1, 1) &= \mathbb{I}_\theta(\boldsymbol{\alpha})(2, 2) = m_h + m_b + m_l \\
\mathbb{I}_\theta(1, 2) &= \mathbb{I}_\theta(\boldsymbol{\alpha})(2, 1) = 0 \\
\mathbb{I}_\theta(1, 3) &= \mathbb{I}_\theta(\boldsymbol{\alpha})(3, 1) = m_l((w_b - w_b^{cm}) + w_l^{cm} \cos(\alpha_l)) \\
&\quad - m_h(w_b^{cm} + (w_h - w_h^{cm}) \cos(\alpha_h)) \\
\mathbb{I}_\theta(2, 3) &= \mathbb{I}_\theta(\boldsymbol{\alpha})(3, 2) = -m_l w_l^{cm} \sin(\alpha_l) \\
&\quad - m_h(w_h - w_h^{cm}) \sin(\alpha_h) \\
\mathbb{I}_\theta(3, 3) &= m_l(w_l^{cm})^2 \sin(\alpha_l)^2 + m_h(w_h - w_h^{cm})^2 \sin(\alpha_h)^2 + \\
&\quad I_h + I_b + I_l + m_h(w_b^{cm} + (w_h - w_h^{cm}) \cos(\alpha_h))^2 \\
&\quad + m_l((w_b - w_b^{cm}) + w_l^{cm} \cos(\alpha_l))^2, \\
\mathbb{I}_\alpha(1, 1) &= -m_h(w_h - w_h^{cm}) \cos(\alpha_h) \\
\mathbb{I}_\alpha(1, 2) &= -m_l w_l^{cm} \cos(\alpha_l) \\
\mathbb{I}_\alpha(2, 1) &= -m_h(w_h - w_h^{cm}) \sin(\alpha_h) \\
\mathbb{I}_\alpha(2, 2) &= m_l w_l^{cm} \sin(\alpha_l) \\
\mathbb{I}_\alpha(3, 1) &= m_h(w_h - w_h^{cm})(w_h - w_h^{cm} + w_b^{cm} \cos(\alpha_h)) \\
\mathbb{I}_\alpha(3, 2) &= -m_l w_l^{cm}(w_l^{cm} + (w_b - w_b^{cm} \cos(\alpha_l)))
\end{aligned}$$

$$\mathbf{D}_\alpha(\boldsymbol{\alpha}) = \begin{pmatrix} m_h(w_h - w_h^{cm})^2 - I_h & 0 \\ 0 & m_l(w_l^{cm})^2 + I_l \end{pmatrix}$$

$$\mathbf{C}_\alpha(1) = 2m_h w_b^{cm} \sin(\alpha_h)(w_h - w_h^{cm})(P^2/Q^2)$$

$$\mathbf{C}_\alpha(2) = 2m_l w_l^{cm} \sin(\alpha_l)(w_b - w_b^{cm})(P^2/Q^2)$$

$$\begin{aligned}
P &= w_l^{cm} \dot{\alpha}_l (m_b m_l (w_l^{cm} + (w_b - w_b^{cm}) \cos(\alpha_l)) + \\
&\quad m_h m_l (w_l^{cm} + (w_h - w_h^{cm}) \cos(\alpha_h + \alpha_l) + w_b \cos(\alpha_l))) \\
&\quad + \dot{\alpha}_h (m_b m_l (w_h - w_h^{cm}) (-w_h - w_h^{cm}) - w_b^{cm} \cos(\alpha_h)) + \\
&\quad m_h m_l ((w_h - w_h^{cm})^2 - (w_h - w_h^{cm})(w_l^{cm} \cos(\alpha_h + \alpha_l) \\
&\quad + w_b \cos(\alpha_h)))
\end{aligned}$$

$$\begin{aligned}
Q &= m_b m_h (w_b^{cm} (w_b^{cm} + 2(w_h - w_h^{cm}) \cos(\alpha_h)) + \\
&\quad (w_h - w_h^{cm})^2) + m_b m_l (w_l^{cm} (w_l^{cm} + 2(w_b - w_b^{cm}) \cos(\alpha_l)) + \\
&\quad (w_b - w_b^{cm})^2) + m_h m_l ((w_h - w_h^{cm})^2 + 2w_b w_l^{cm} \cos(\alpha_l) + \\
&\quad 2w_b (w_h - w_h^{cm}) \cos(\alpha_h) + 2w_l^{cm} (w_h - w_h^{cm}) \cos(\alpha_l + \alpha_h))
\end{aligned}$$

REFERENCES

- [1] Evan Chang-Siu, Thomas Libby, Masayoshi Tomizuka, and Robert J Full. A lizard-inspired active tail enables rapid maneuvers and dynamic stabilization in a terrestrial robot. In *IEEE/RSJ International Conference on Intelligent Robots and Systems (IROS)*, pages 1887–1894. IEEE, 2011.
- [2] Thomas William Mather and Mark Yim. Modular configuration design for a controlled fall. In *IEEE/RSJ International Conference on Intelligent Robots and Systems (IROS)*, pages 5905–5910. IEEE, 2009.
- [3] Jeffrey T Bingham, Jeongseok Lee, Ravi N Haksar, Jun Ueda, and C Karen Liu. Orienting in mid-air through configuration changes to achieve a rolling landing for reducing impact after a fall. In *IEEE/RSJ International Conference on Intelligent Robots and Systems (IROS)*, pages 3610–3617. IEEE, 2014.

- [4] Jianguo Zhao, Tianyu Zhao, Ning Xi, Matt W Mutka, and Li Xiao. Msu tailbot: Controlling aerial maneuver of a miniature-tailed jumping robot. *Mechatronics, IEEE/ASME Transactions on*, 20(6):2903–2914, 2015.
- [5] Aaron M Johnson, Thomas Libby, and Evan Chang-Siu. Tail assisted dynamic self righting. In *Proceedings of the Fifteenth International Conference on Climbing and Walking Robots*, pages 611–620.
- [6] TR Kane and MP Scher. A dynamical explanation of the falling cat phenomenon. *International Journal of Solids and Structures*, 5(7):663–IN2, 1969.
- [7] Richard Montgomery. Gauge theory of the falling cat. *Fields Institute Communications*, 1, 1993.
- [8] Elie A Shammass, Howie Choset, and Alfred A Rizzi. Towards a unified approach to motion planning for dynamic underactuated mechanical systems with non-holonomic constraints. *The International Journal of Robotics Research*, 26(10):1075–1124, 2007.
- [9] Ross L Hatten and Howie Choset. Geometric motion planning: The local connection, stokes theorem, and the importance of coordinate choice. *The International Journal of Robotics Research*, 30(8):988–1014, 2011.
- [10] Anthony M Bloch, Mahmut Reyhanoglu, and N Harris McClamroch. Control and stabilization of nonholonomic dynamic systems. *IEEE Transactions on Automatic Control (TAC)*, 37(11):1746–1757, 1992.
- [11] Gregory C Walsh and S Shankar Sastry. On reorienting linked rigid bodies using internal motions. *IEEE Transactions on Robotics and Automation (TRA)*, 11(1):139–146, 1995.
- [12] Mahmut Reyhanoglu and N Harris McClamroch. Planar reorientation maneuvers of space multibody systems using internal controls. *Journal of guidance, control, and dynamics*, 15(6):1475–1480, 1992.
- [13] Cliff Frohlich. Do springboard divers violate angular momentum conservation? *American Journal of Physics*, 47(7):583–592, 1979.
- [14] Wayne L Wooten and Jessica K Hodgins. Animation of human diving. In *Computer Graphics Forum*, volume 15, pages 3–13. Wiley Online Library, 1996.
- [15] Lara S Crawford and S Shankar Sastry. Biological motor control approaches for a planar diver. In *IEEE International Conference on Decision and Control (CDC)*, volume 4, pages 3881–3886, 1995.
- [16] J-M Godhavn, Andrea Balluchi, Lara S Crawford, and S Shankar Sastry. Steering of a class of nonholonomic systems with drift terms. *Automatica*, 35(5):837–847, 1999.
- [17] Robert R Playter and Marc H Raibert. Control of a biped somersault in 3d. In *Intelligent Robots and Systems, 1992., Proceedings of the 1992 IEEE/RSJ International Conference on*, volume 1, pages 582–589. IEEE, 1992.
- [18] Marcus G Pandy, Felix E Zajac, Eunsup Sim, and William S Levine. An optimal control model for maximum-height human jumping. *Journal of biomechanics*, 23(12):1185–1198, 1990.
- [19] Emanuel Todorov. Optimality principles in sensorimotor control. *Nature neuroscience*, 7(9):907–915, 2004.
- [20] Juanita V Albro, Garrett A Sohl, James E Bobrow, and Frank C Park. On the computation of optimal high-dives. In *Robotics and Automation, 2000. Proceedings. ICRA'00. IEEE International Conference on*, volume 4, pages 3958–3963. IEEE, 2000.
- [21] James E Bobrow, B Martin, G Sohl, EC Wang, Frank C Park, and Junggon Kim. Optimal robot motions for physical criteria. *Journal of Robotic systems*, 18(12):785–795, 2001.
- [22] Jens Koschorreck and Katja Mombaur. Modeling and optimal control of human platform diving with somersaults and twists. *Optimization and Engineering*, 13(1):29–56, 2012.
- [23] JT Betts and I Kolmanovskiy. Practical methods for optimal control using nonlinear programming. *Applied Mechanics Reviews*, 55:68, 2002.
- [24] MATLAB. *version 8.3.0 (R2015b)*. The MathWorks Inc., Natick, Massachusetts, 2015.